

Free Energy Profile of the Reaction between the Hydroxide Ion and Ethyl Acetate in Aqueous and Dimethyl Sulfoxide Solutions: A Theoretical Analysis of the Changes Induced by the Solvent on the Different Reaction Pathways

Josefredo R. Pliego, Jr.,^{*,†} and José M. Riveros[‡]

Departamento de Química, Universidade Federal de Santa Catarina, CEP 88040-900 Florianópolis, SC, Brazil, and Instituto de Química, Universidade de São Paulo, Avenida Lineu Prestes 748, CEP 05508-900 São Paulo, SP, Brazil

Received: October 2, 2003; In Final Form: January 14, 2004

An extensive analysis of the free energy profile for the reaction of the hydroxide ion with ethyl acetate in both aqueous and dimethyl sulfoxide (DMSO) solutions has been carried out using ab initio calculations and including the solvent effect by the polarizable continuum model. Different reaction pathways were investigated, such as the usual B_{AC}2 mechanism, the carbanion mechanism, the elimination mechanism, and the S_N2 mechanism. Our calculation agrees with the view that in aqueous and DMSO solution basic hydrolysis occurs by the B_{AC}2 mechanism. In water, the predicted activation free energy value is 17.6 kcal mol⁻¹, which is in very good agreement with the experimental value of 18.8 kcal mol⁻¹. Using a new parametrization of the polarizable continuum model adequate to describe anions and neutral species in DMSO, the present study predicts a rate enhancement by a factor of 435 in the reaction when going from water (protic solvent) to DMSO (dipolar aprotic solvent). In this solvent, the activation free energy is predicted to drop to 14.0 kcal mol⁻¹. Furthermore, our results point out that the elimination mechanism is only 6.0 kcal mol⁻¹ ($\Delta G_{\text{sol}}^{\ddagger} = 20.0$ kcal mol⁻¹) less favorable than the B_{AC}2 mechanism in DMSO solution, and 8.4 kcal mol⁻¹ less favorable in water. The S_N2 and the carbanion mechanisms have barriers above 30 kcal mol⁻¹ in water and DMSO and are thus highly unfavorable. These results suggest the elimination mechanism can become the dominant pathway in the basic hydrolysis of sterically crowded esters at the carbonyl center.

I. Introduction

A set of chemical reagents are often found to undergo reactions through competing pathways that lead to different products. This consideration is particularly critical in the development of synthetic routes because side reactions can lead to substantial reduction of the yield of the target products.¹ Thus, the development of methods, procedures, reactants, or catalysts that are able to control the generation of the final product is of utmost importance. The first step in this direction is to understand the reaction mechanism, other possible reaction pathways, and the influence of the solvent and the temperature on each pathway. Nowadays, some of these questions can be addressed by theoretical calculations. Indeed, in recent years important studies aimed to provide a general view of a determined reaction system or address specific mechanistic questions have been reported.^{2–21}

The objective of this work is to provide a general view of a classical reaction system: the interaction of the hydroxide ion with ethyl acetate. This is a representative system and can provide us with quantitative insights on the activation barriers and the thermodynamic stabilities of the different reaction pathways and products. Theoretical studies dealing with the basic hydrolysis of esters both in the gas phase and in aqueous solution have been reported in the literature.^{5–10,22–25} Jorgensen pioneered the study of the gas phase reaction of the hydroxide

ion with methyl formate that resulted in a careful analysis of the reaction pathways.²⁵ Subsequent theoretical studies mainly emphasized the B_{AC}2 and S_N2 mechanisms for different esters.^{5–9,24} However, recently, an extensive study of the reaction pathways of the basic hydrolysis of methyl formate both in the gas phase and in aqueous solution was reported by Pliego and Riveros.^{10,22} In that work, the authors used a hybrid discrete/continuum approach to solvation^{26,27} in order to calculate the free energy profile for the reaction in aqueous solution. The calculated rate constant and thermodynamic parameters were found to be in excellent quantitative agreement with the experimental values.

In the present article, we have studied the reaction between the hydroxide ion and ethyl acetate in two different solvents: water and dimethyl sulfoxide (DMSO) solutions. This reaction^{28–30} has been reported to display the classical enhancement observed in S_N2 reactions when going from protic to dipolar aprotic solvents.³¹ To model this important effect, we have used our recent parametrization of the polarizable continuum (PCM) model capable of reproducing the solvation free energy of anions in DMSO with good accuracy.^{32,33} Thus, our theoretical study is concerned with the evaluation of the rate enhancement of basic ester hydrolysis in going from protic (water) to dipolar aprotic (DMSO) solvent and the prediction of the relative importance of the competing pathways.

II. Reaction Pathways

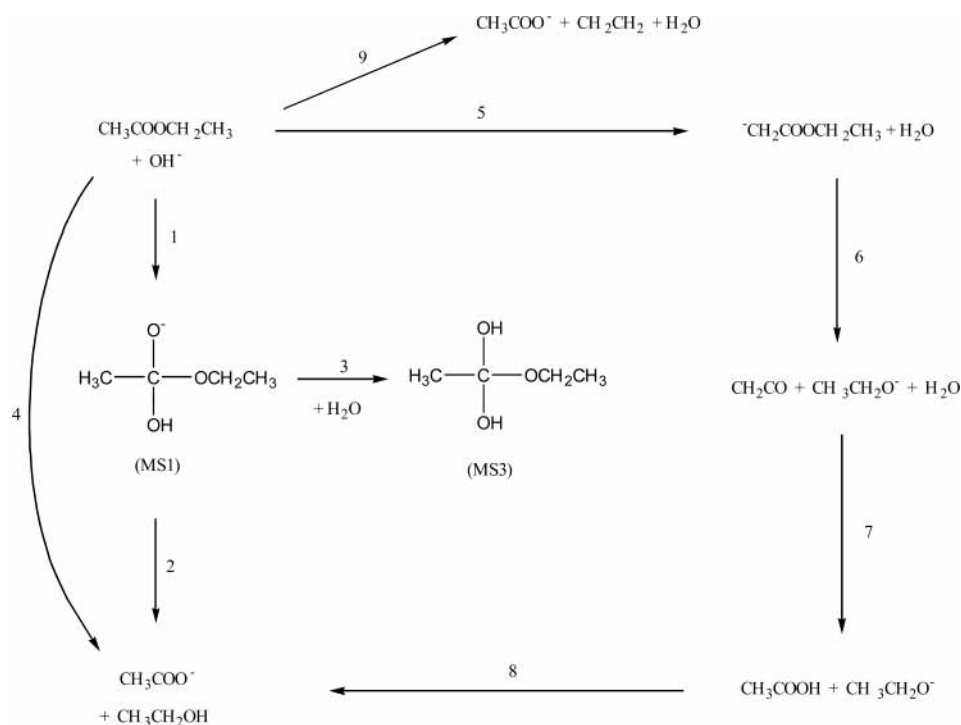
It is well established that the usual pathway for the hydroxide ion reaction with carboxylic esters, in aqueous solution, takes

* Corresponding author. Current address: Departamento de Química, CFM, Universidade Federal de Santa Catarina, CEP 88040-900 Florianópolis, SC, Brazil. E-mail: josef@qmc.ufsc.br.

† Universidade Federal de Santa Catarina.

‡ Universidade de São Paulo. E-mail: jmmigra@iq.usp.br.

SCHEME 1



place through the B_{AC}2 mechanism, where the hydroxide ion attacks the carbonyl carbon, leading to a tetrahedral intermediate. In the following step, this species decomposes to the carboxylate and alcohol products.^{34–39} Nevertheless, several other possible pathways could be considered for this system, and they are summarized in Scheme 1. In this scheme, steps 1 and 2 correspond to the B_{AC}2 mechanism, whereas step 3 represents the protonation of the tetrahedral intermediate by a water molecule. Step 4 is the S_N2 mechanism corresponding to the nucleophilic attack of the hydroxide ion on the ethyl group. Step 5 is the proton abstraction leading to the enolate ion. This anion can decompose through elimination of ethoxide and formation of a ketene (step 6) that can further react with water to generate acetic acid and ethoxide (step 7). The last step of this pathway is the acid–base reaction of step 8. This carbanion mechanism was proposed to take place in some cases.⁴⁰ Finally, step 9 corresponds to the elimination mechanism leading to acetate, ethene, and water. It should be noted that the enolate could also react by an aldol condensation type reaction with ethyl acetate, but this possibility was not explored in this work.

III. Theoretical Calculations

The potential energy surfaces for the interaction of the hydroxide ion with ethyl acetate were explored at the HF/6-31+G(d) level of theory, and the nature of the stationary points was characterized by harmonic frequency calculations. The optimized structures were then used to make single point calculations at the MP2 level of electron correlation using the 6-311+G(2df,2p) basis set. Although a high level of accuracy would require the use of more demanding methods such as MP4 or CCSD(T), we think that the present level of theory is adequate for our objectives.

To include solvent effects, we have used the polarizable continuum model of Tomasi and co-workers^{41–45} in conjunction with the HF/6-31+G(d) wave function. There are many versions of this method, differing in the definition of the cavity and in the treatment of the charges lying outside of the cavity. We

have preferred to use fixed atomic radii for H (1.20 Å), O (1.50 Å), and C (1.70 Å) and a scale factor of 1.20 that is adequate for aqueous solution.⁴⁶ It should be noted that the use of a combined discrete/continuum solvation model is more accurate to describe ions in aqueous solution, as it was shown in a recent study by Pliego and Riveros.^{26,27} An alternative approach would be to use the PCM–UAHF model,⁴³ the default method in Gaussian 98. However, this method was parametrized to describe the solvation of usual functional groups, using a small set of solvation data, and may thus not be appropriated to describe the solvation of transition states. Indeed, in a recent study on the basic hydrolysis of β-lactams, Massova and Kollman have estimated the activation free energy of the basic hydrolysis of *N,N*-dimethylacetamide using the PCM–UAHF model. The value obtained by these authors, based on the stability of the tetrahedral intermediate, is ~28.7 kcal mol⁻¹ and should be compared with the value of 24.1 kcal mol⁻¹ reported by Guthrie⁴⁷ that was derived from experimental data. By comparison, a recent kinetic study by Brown and co-workers^{48,49} on the basic hydrolysis of formamide has resulted in an activation free energy barrier of 21.2 kcal mol⁻¹. Thus, it seems that the PCM–UAHF model overestimates the differential solvation between the transition state and the reactants, leading to higher activation barriers.

For solvation in DMSO solution, we have also used the PCM model with fixed atomic cavities. Many authors have made use of continuum models to describe solvation in organic solvents using the dielectric constant of the solvent, but adopting the same cavities that were optimized for water. This approach is incorrect because these continuum models would then predict that different solvents with high dielectric constants have the same solvation ability. Consequently, the rate enhancement observed when the reaction goes from protic to dipolar aprotic solvents would not be observed.³¹ To overcome this problem, a different cavity size must be defined. For DMSO solution, Pliego and Riveros have reported the first parametrization of the PCM model to describe solvation of anions in DMSO, an

approach that can also be applied to neutral species.³³ This parametrization is adequate to describe anion–molecule reactions, and its good accuracy can be confirmed by a recent calculation of the pK_a 's of over 41 organic acids in DMSO solution.⁵⁰ The rms error in that study was only 2.2 pK_a units. This parametrization of the PCM model for DMSO uses the following atomic radii: H (1.20 Å), O (1.50 Å), and C (1.70 Å), with a scale factor of 1.35.

The gas phase thermodynamic properties were calculated using the ab initio data and standard statistical mechanics formulas.⁵¹ All contributions, namely, translational, rotational, vibrational, and electronic, were included. The gas phase reaction and activation Gibbs free energy (ΔG_g^*) was added to the difference of the solvation free energy ($\Delta\Delta G_{\text{solv}}^*$) in order to calculate the solution phase Gibbs free energy (ΔG_{sol}^*):

$$\Delta G_{\text{sol}}^* = \Delta G_g^* + \Delta\Delta G_{\text{solv}}^*$$

It is worthwhile to mention that some of the optimized transition state structures are not true transition states in the *gas phase*. Thus, structures TS1 and TS6 are not maxima on the gas phase reaction path. In this situation, we have optimized several structures by freezing different C–O distances, in the gas phase, and added the solvation free energy in order to obtain the potential of mean force surface. On this surface, a maximum on the reaction path can be observed and we have taken these structures as the transition state for the liquid phase reaction. The vibrational contribution to the gas phase thermodynamic properties of these structures is then calculated using the Hessian projection method of Miller et al.⁵²

The ab initio HF and MP2 calculations were performed with the Gaussian 94 program system,⁵³ and the calculations of solvation free energies were done with the Gamess program system.⁵⁴ The boundary element method (BEM) formulation of the PCM model was used for aqueous solution, while for DMSO we have used the integral equation formalism (IEF) routine. Corrections for the escape charges were included in both calculations. Finally, it should be made clear that we are using 1 mol L⁻¹ as the standard state for both the gas phase and the solution for all thermodynamic properties.

IV. Results

The structures for the optimized transition states are shown in Figure 1, while Figures 2 and 3 display the calculated free energy profiles in water and DMSO solutions. The calculated solvation free energies and the reaction and activation thermodynamic properties are tabulated in Tables 1 and 2, respectively. Each step indicated in the tables is numbered in accordance with Scheme 1, and the transition state structures are named in accordance with these steps. Thus, step 1 in this scheme corresponds to transition state TS1, step 2, to TS2, and so on. For some steps, the transition states were not calculated because in these cases our interest was to evaluate the thermodynamic feasibility of the reaction.

Free Energy Profile in Aqueous Solution. The activation barrier in step 1, corresponding to the nucleophilic attack of the hydroxide ion to the carbonyl carbon (TS1), is calculated to be 17.6 kcal mol⁻¹. This value is in very good agreement with the experimental one⁵⁵ of 18.8 kcal mol⁻¹. This small error is somewhat unexpected because the calculated solvation free energy of the hydroxide ion, -92.5 kcal mol⁻¹, underestimates the experimental one (-105.0 kcal mol⁻¹)³² by 12.5 kcal mol⁻¹. However, the PCM method also underestimates the ΔG_{solv}^* of

alkoxides by a similar value, and as a consequence, the differential solvation effect of 27.5 kcal mol⁻¹ must be reliable.

The tetrahedral intermediate (MS1) is 9.2 kcal mol⁻¹ above the reactants, very similar to the calculated value of 8.1 kcal mol⁻¹ for the OH⁻ + HCOOCH₃ system.¹⁰ The next step, elimination of ethanol through TS2, has a barrier of 8.8 kcal mol⁻¹, and it is 18.0 kcal mol⁻¹ above the reactants. On the basis of our previous work,¹⁰ the decomposition of the tetrahedral intermediate should occur either by direct elimination of an ethoxide ion, explicitly solvated by two water molecules, or by a catalyzed mechanism involving a second water molecule, as shown by other authors,^{6,7} due to the fact that these pathways have a lower barrier. We have not analyzed this possibility in this work, since it involves the use of additional water molecules, and our present objective is to provide a comparison with the reaction in anhydrous DMSO. Nevertheless, it is reasonable to assume that the barrier of 17.6 kcal mol⁻¹ determines the kinetics in aqueous solution by this reaction pathway. The final products, ethanol plus acetate, are 20.8 kcal mol⁻¹ below the reactants. This value is probably overestimated because the solvation free energy calculated for the acetate ion underestimates the experimental one by only 4.6 kcal mol⁻¹. We have taken gas phase ΔH_f° data from the NIST⁵⁶ compilation and theoretically calculated entropy and experimental solvation free energy data from our recent report³² in order to evaluate the reaction ΔG_{sol}^* for steps 1 and 2. The obtained value is -14.6 kcal mol⁻¹, indicating an error of 6 kcal mol⁻¹ in our theoretical ab initio PCM calculation. This error is expected because the PCM method predicts more reliable solvation free energies for carboxylate ions than for alkoxides.

The tetrahedral intermediate can be protonated (step 3) with a reaction free energy of 13.1 kcal mol⁻¹. This value allows us to predict the pK_a of the neutral tetrahedral intermediate as being 6.1 units through a previously described method.²⁶ Thus, protonation does not take place in alkaline solution and this step was not included in the free energy profile.

The S_N2 mechanism, represented by TS4, has a $\Delta G_{\text{sol}}^{\ddagger}$ of 34.7 kcal mol⁻¹, considerably higher than that of the B_{AC}2 mechanism. Therefore, this pathway can be ruled out for this system.

Another possible reaction path is the formation of the enolate ion in step 5. The activation $\Delta G_{\text{sol}}^{\ddagger}$ is 14.7 kcal mol⁻¹, below that of step 1. However, the enolate is 7.1 kcal mol⁻¹ above the free energy of the reactants, and the following step (TS6), corresponding to the carbanion mechanism of ester hydrolysis, has an overall free energy barrier of 37.3 kcal mol⁻¹. Thus, this mechanism can be ruled out for this reaction system. The next steps, 7 and 8, correspond to the hydration of ketene formed in step 6 followed by an acid–base reaction, leading to the final products: ethanol plus acetate.

The last step, step 9, is the elimination mechanism represented by structure TS9. This mechanism has a predicted activation free energy of 26.0 kcal mol⁻¹, and the products are predicted to be stable by 20.4 kcal mol⁻¹. This higher barrier implicates that this pathway is also unfavorable for ethyl acetate.

Free Energy Profile in DMSO Solution. The DMSO solvent has a lower ability to solvate anions, mainly small and charge localized anions. A consequence of this fact is that all structures, intermediates, products, and transition states are stabilized in relation to the reactants when going from water to DMSO solution. This becomes noticeable in Figures 2 and 3, where the free energy profiles are very similar.

In step 1 (B_{AC}2 mechanism) the activation barrier has decreased to 14.0 kcal mol⁻¹, a variation of -3.6 kcal mol⁻¹. The free energy of intermediate MS1 is 5.1 kcal mol⁻¹ above that

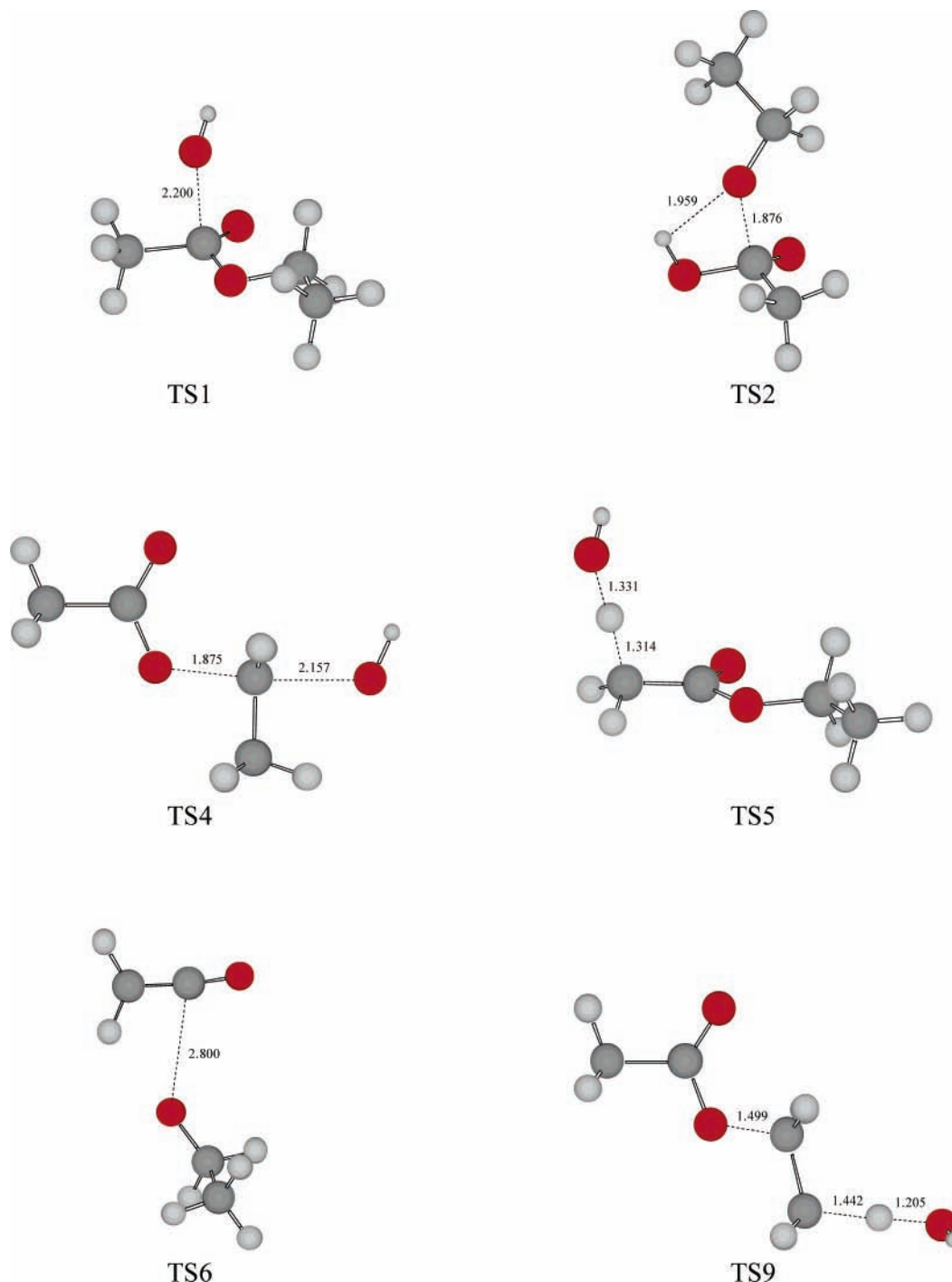


Figure 1. Transition states for the $\text{OH}^- + \text{CH}_3\text{COOCH}_2\text{CH}_3$ reaction system.

of the reactants, and the transition state of the following step (TS2) has a free energy below that of TS1, amounting only to $13.3 \text{ kcal mol}^{-1}$. Thus, there is an inversion of the barrier height in relation to the case of aqueous solution. The products are stable by $23.8 \text{ kcal mol}^{-1}$. The experimental free energy value for this reaction can be calculated using experimental data, as was done for the water solution case. However, due to the lack of solvation data of ethyl acetate in DMSO, we have used our theoretical estimate of $-4.0 \text{ kcal mol}^{-1}$. The calculated value in DMSO is $-25.2 \text{ kcal mol}^{-1}$, in very good agreement with our ab initio PCM calculation of $-23.8 \text{ kcal mol}^{-1}$. The error of only $1.4 \text{ kcal mol}^{-1}$ is expected because previous studies⁵⁰ have shown that our parametrization³³ of the PCM model for DMSO is reliable. Step 3 was only considered for water solution,

while step 4, the $\text{S}_{\text{N}}2$ mechanism, remains with a high barrier: $30.5 \text{ kcal mol}^{-1}$. Consequently, this pathway is also not important in DMSO solution.

The enolate can be easily formed in step 5 with an activation $\Delta G_{\text{sol}}^\ddagger$ of $9.4 \text{ kcal mol}^{-1}$ and lies only $2.9 \text{ kcal mol}^{-1}$ above the reactants. The elimination of ethoxide and formation of ketene (step 6) with a barrier of $33.2 \text{ kcal mol}^{-1}$ makes this pathway unfavorable. Finally, the elimination mechanism (step 9) has a barrier of only 20 kcal mol^{-1} , about 6 kcal mol^{-1} below that barrier in aqueous solution.

V. Discussion

Our calculation for this system predicts that in aqueous solution the reaction takes place by the $\text{B}_{\text{AC}}2$ mechanism, in

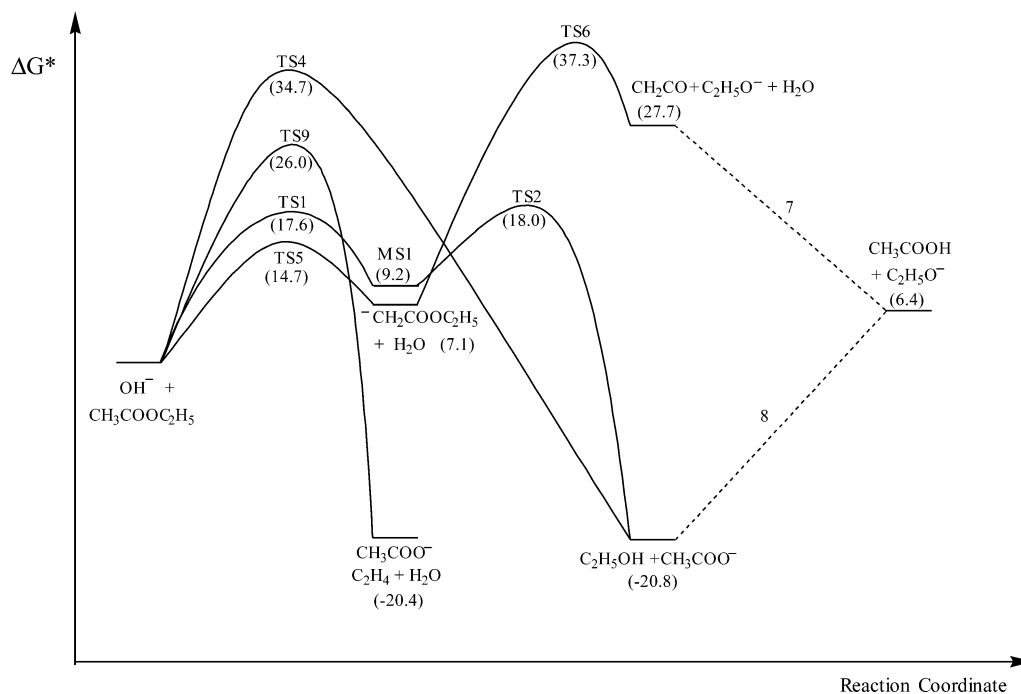


Figure 2. Free energy profile of the $\text{OH}^- + \text{CH}_3\text{COOC}_2\text{H}_5$ reaction in aqueous solution. Units of kilocalories per mole.

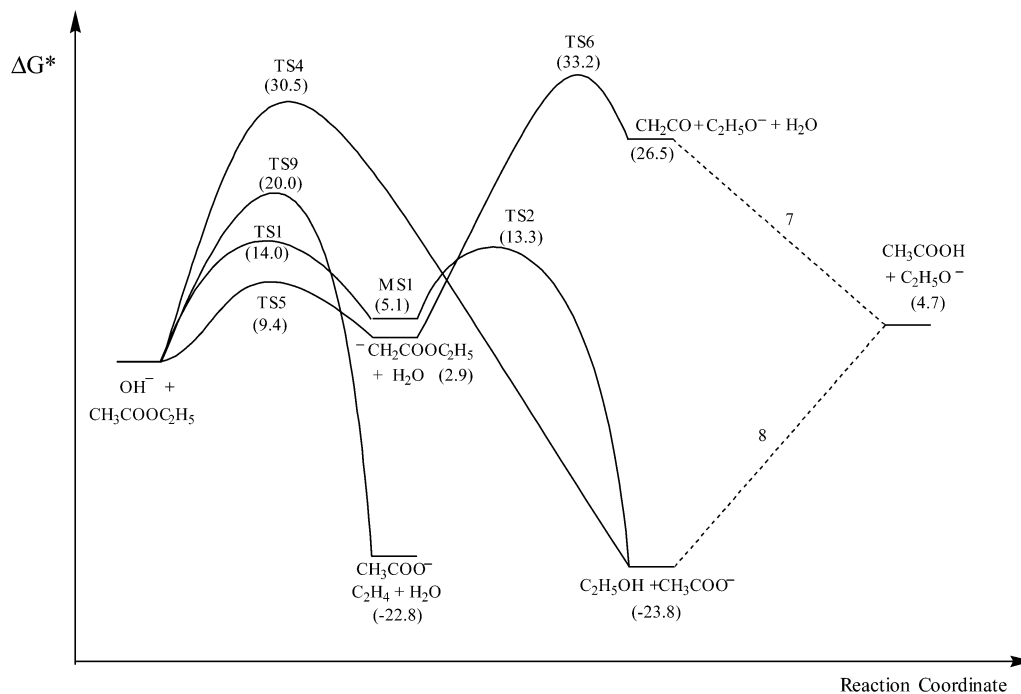


Figure 3. Free energy profile of the $\text{OH}^- + \text{CH}_3\text{COOC}_2\text{H}_5$ reaction in DMSO solution. Units of kilocalories per mole.

agreement with the experimental studies on basic ester hydrolysis. Furthermore, our results point out that parallel reactions do not take place because the respective barriers are very high. Similarly, in DMSO solution the $\text{B}_{\text{AC}2}$ mechanism dominates, but the elimination mechanism (TS9) is only 6 kcal mol⁻¹ less favorable than it is in water solution (8.4 kcal mol⁻¹). This result is in agreement with a general rule that establishes that a less polar (or solvating) medium favors elimination.⁵⁷ In addition, regarding this relatively favorable elimination mechanism, a recent experimental study has shown that an enzyme of *Staphylococcus aureus* inactivates the Streptogramin B antibiotics through an elimination mechanism involving an ester group.⁵⁸ This result shows that less favorable reaction pathways can play

an important role in biochemistry and a proper evaluation of the respective activation barriers is relevant.

The decrease of the barrier for step 1 in going from water to DMSO predicted by the present calculations is 3.6 kcal mol⁻¹. This corresponds to a rate enhancement by a factor of 435. The available kinetics data in DMSO–water mixtures and pure water provide a rate enhancement from water (0.110 L mol⁻¹ s⁻¹)⁵⁵ to 55% aqueous DMSO (0.529 L mol⁻¹ s⁻¹)³⁰ by a factor of 5. This value is probably much smaller than that for going directly to pure DMSO, because the high concentration of water in the 55% aqueous DMSO solution can lead to specific solvation of the hydroxide ion and the rate constant becomes close to the aqueous phase value. Typically, the factors for protic to dipolar

TABLE 1: Calculated Solvation Free Energies^a

species	ΔG_{solv}^* (water)	ΔG_{solv}^* (DMSO)
OH ⁻	-92.45	-82.08
H ₂ O	-6.79	-4.97
CH ₃ COOCH ₂ CH ₃	-6.24	-3.97
CH ₃ CH ₂ O ⁻	-76.63	-68.15
CH ₃ CH ₂ OH	-4.97	-3.38
CH ₂ CO	-3.08	-1.98
CH ₃ COO ⁻	-72.74	-64.72
CH ₃ COOH	-7.23	-4.78
C ₂ H ₄	-1.21	-0.86
MS1	-68.05	-59.52
MS2	-65.92	-59.31
MS3	-7.20	-4.65
TS1	-71.19	-62.18
TS2	-63.17	-55.26
TS4	-66.94	-58.55
TS5	-68.45	-61.14
TS6	-63.68	-56.96
TS9	-64.99	-58.41

^a Units of kilocalories per mole. Ab initio calculations at the PCM/HF/6-31+G(d) level. Standard state of 1 mol L⁻¹.

aprotic rate enhancement involving hard nucleophiles³¹ are around 10³ to 10⁷, corresponding to a 4.1 to 9.5 kcal mol⁻¹ decrease in the activation barrier. Our calculation predicts a value close to this interval.

The present information on the free energy profile of this reaction allows us to make some extrapolations for more general situations. An example is the case of sterically hindered esters around the carbonyl center. In these cases, it is probable that the barrier for the B_{AC}2 mechanism becomes very high, and parallel pathways can become important. On the basis of our calculations, the elimination mechanism is the most viable process. In DMSO solution, we have predicted a $\Delta G_{\text{sol}}^\ddagger$ of only 20 kcal mol⁻¹, in comparison to 26 kcal mol⁻¹ in water. Thus, even at room temperature the reaction could take place in DMSO easily, while in water it would take place slowly. On the other hand, for esters where the elimination mechanism is not possible,

the second most viable alternative is the S_N2 mechanism. However, even in DMSO the barrier is 30.5 kcal mol⁻¹, indicating that this process becomes favorable only at higher temperature. In spite of this, some authors have used the S_N2 reaction with iodide to cleave esters.⁵⁹

We can also infer the free energy profile of the reaction of alkoxides with ethyl acetate in DMSO, since they should display similar reactivities to that of the hydroxide ion. In this case, the B_{AC}2 mechanism would lead only to the exchange of the alkoxide and the most likely reaction pathway is the elimination mechanism. Nevertheless, other possibilities need to be considered: the aldol condensation type reaction of the enolate formed in step 5 with another ester molecule. The importance of this pathway will depend mainly on the activation barrier for the condensation step, because in DMSO the enolate is predicted to be only 2.9 kcal mol⁻¹ less stable than the reactants and the alcohols have a pK_a in DMSO close to the pK_a of water.⁶⁰

The basic hydrolysis of ethyl acetate by the B_{AC}2 mechanism in water solution has also been studied theoretically by Zhan et al.²⁴ These authors did not calculate the activation free energy but did calculate the energy barrier for the liquid phase reaction using different continuum models. The barrier was evaluated as the sum of the MP2/6-31++G(d,p) gas phase energies (including zero point vibrational energy) with the solvation free energy calculated by the continuum model. We can compare their results with the present one by adding the entropic contribution ($-T\Delta S_g^\ddagger = 6.9$ kcal mol⁻¹, our calculation) to the Zhan et al.²⁴ computed barriers in solution. Thus, for their SVPE method, the free energy barriers are in the range 13.5 kcal mol⁻¹ (0.001 au of isodensity) to 17.3 kcal mol⁻¹ (0.002 au of isodensity), while, for the PCM and IEFPCM methods with UAHF cavities, the barriers are in the range 21.0–23.8 kcal mol⁻¹. From these results, it is evident that the PCM based methods using UAHF cavities overestimate the experimental barrier, while the SVPE method with a cavity defined by a value of 0.001 au of isodensity leads to an underestimated ΔG^\ddagger . On

TABLE 2: Thermodynamic Properties for the Activation and Reaction Steps Shown in Scheme 1^a

step	Activation Properties									
	gas phase						aqueous solution		DMSO solution	
	MP2 ^b	ΔZPE^c	ΔE^d	ΔH_g^\ddagger	ΔS_g^\ddagger	ΔG_g^\ddagger	$\Delta\Delta G_{\text{solv}}^\ddagger$	$\Delta G_{\text{sol}}^\ddagger$	$\Delta\Delta G_{\text{solv}}^\ddagger$	$\Delta G_{\text{sol}}^\ddagger$
1	-17.57	1.32	-16.25	-16.78	-23.14	-9.88	27.51	17.63	23.87	13.99
2	5.96	-1.65	4.31	4.45	1.64	3.96	4.88	8.84	4.26	8.22
4	-2.39	0.12	-2.27	-2.09	-17.00	2.98	31.75	34.73	27.51	30.49
5	-19.60	-2.05	-21.65	-21.89	-21.41	-15.51	30.25	14.74	24.91	9.40
6	34.62	-4.13	30.49	31.21	10.78	27.99	2.24	30.23	2.36	30.35
9	-9.60	-3.07	-12.67	-12.48	-16.14	-7.67	33.70	26.03	27.64	19.97
step	Reaction Properties									
	gas phase						aqueous solution		DMSO solution	
	MP2 ^b	ΔZPE^c	ΔE^d	ΔH_g^*	ΔS_g^*	ΔG_g^*	$\Delta\Delta G_{\text{solv}}^*$	ΔG_{sol}^*	$\Delta\Delta G_{\text{solv}}^*$	ΔG_{sol}^*
1	-31.99	3.30	-28.69	-29.62	-27.29	-21.48	30.65	9.16	26.54	5.06
2	-7.30	-2.25	-9.55	-9.21	37.17	-20.30	-9.66	-29.95	-8.58	-28.88
3	36.45	0.70	37.15	37.14	-2.56	37.90	-24.81	13.09	-22.25	15.65
4	-39.28	1.05	-38.23	-38.83	9.88	-41.78	20.99	-20.79	17.96	-23.82
5	-17.05	-1.20	-18.25	-18.18	2.50	-18.93	25.99	7.06	21.77	2.85
6	47.86	-4.83	43.03	43.25	29.40	34.49	-13.80	20.68	-10.82	23.67
7	-36.69	6.06	-30.63	-31.78	-26.10	-24.00	2.65	-21.35	2.16	-21.84
8	-33.40	1.02	-32.38	-32.12	4.07	-33.34	6.15	-27.19	4.84	-28.50
9	-23.91	-4.09	-28.00	-27.55	36.13	-38.33	17.95	-20.37	15.51	-22.82

^a Units of kilocalories per mole. Standard state of 1 mol L⁻¹ for both gas phase and liquid phase thermodynamic properties. Correction factors ($-RT \ln(2)$) were included for the enantiomeric minima and the transition state structures. ^b This corresponds to the MP2/6-311+G(2df,2p)//HF/6-31+G(d) level of theory. ^c Zero point vibrational energy contribution. ^d Sum of the MP2 energy plus the change of the zero point energy (ΔZPE) contribution.

the other hand, the use of an isodensity of 0.002 au to define the cavity results in a ΔG^\ddagger close to our computed value of 17.6 kcal mol⁻¹, which is in good agreement with the experimental data. Zhan et al.²⁴ have argued that this smaller cavity is justified due to the strong hydrogen bond present in this system.

VI. Conclusion

Our theoretical calculations predict that the basic hydrolysis of ethyl acetate takes place through the B_{AC}2 mechanism in both aqueous and DMSO solutions. The theoretical activation free energy barrier for this pathway decreases from 17.6 to 14.0 kcal mol⁻¹ in going from water to DMSO. Thus, the basic hydrolysis of esters presents the very well-known rate enhancement observed in S_N2 reactions upon the transfer of the reaction from protic to dipolar aprotic solvent. The elimination mechanism is the second alternative with activation free energy barriers of 26.0 kcal mol⁻¹ (water) and 20.0 kcal mol⁻¹ (DMSO). This pathway could be important in the basic hydrolysis of esters sterically hindered on the carbonyl group.

Acknowledgment. The authors thank the Brazilian Research Council (CNPq) for support through the Profix program (J.R.P., Jr.) and for a senior research fellowship (J.M.R.). The authors also thank the FAPESP for support.

Supporting Information Available: Tables of thermodynamic properties of the reaction of OH⁻ and CH₃COOCH₂CH₃ in water or in DMSO solution and tables of structure parameters for the tetrahedral intermediates and the transition states. This material is available free of charge via the Internet at <http://pubs.acs.org>.

References and Notes

- Repic, O.; Prasad, K.; Lee, G. T. *Org. Process Res. Dev.* **2001**, *5*, 519.
- Chandrasekhar, J.; Shariffsukul, S.; Jorgensen, W. L. *J. Phys. Chem. B* **2002**, *106*, 8078.
- Dejaegere, A.; Liang, X.; Karplus, M. *J. Chem. Soc., Faraday Trans.* **1994**, *90*, 1763.
- Kahn, K.; Bruce, T. C. *J. Phys. Chem. B* **2003**, *107*, 6876.
- Zhan, C.-G.; Landry, D. W.; Ornstein, R. L. *J. Am. Chem. Soc.* **2000**, *122*, 1522.
- Zhan, C.-G.; Landry, D. W.; Ornstein, R. L. *J. Am. Chem. Soc.* **2000**, *122*, 2621.
- Haeffner, F.; Hu, C.-H.; Brinck, T.; Norin, T. *THEOCHEM* **1999**, *459*, 85.
- Tantillo, D. J.; Houk, K. N. *J. Org. Chem.* **1999**, *64*, 3066.
- Pranata, J. *J. Phys. Chem.* **1994**, *98*, 1180.
- Pliego, J. R., Jr.; Riveros, J. M. *Chem.—Eur. J.* **2002**, *8*, 1945.
- Pliego, J. R., Jr.; Riveros, J. M. *J. Phys. Chem. A* **2002**, *106*, 371.
- Cuccovia, I. M.; Silva, M. A.; Ferraz, H. M. C.; Pliego, J. R., Jr.; Riveros, J. M.; Chaimovich, H. *J. Chem. Soc., Perkin Trans. 2* **2000**, 1896.
- Pliego, J. R., Jr.; de Almeida, W. B. *J. Phys. Chem. A* **1999**, *103*, 3904.
- Pliego, J. R., Jr.; de Almeida, W. B. *J. Phys. Chem.* **1996**, *100*, 12410.
- Lopez, X.; Mujika, J. I. A.; Blackburn, G. M.; Karplus, M. *J. Phys. Chem. A* **2003**, *107*, 2304.
- Bakowies, D.; Kollman, P. A. *J. Am. Chem. Soc.* **1999**, *121*, 5712.
- Massova, I.; Kollman, P. A. *J. Phys. Chem. B* **1999**, *103*, 8628.
- O'Brien, J. F.; Pranata, J. *J. Phys. Chem.* **1995**, *99*, 12759.
- Wu, Z. J.; Ban, F. Q.; Boyd, R. J. *J. Am. Chem. Soc.* **2003**, *125*, 3642.
- Bernardi, F.; Bongini, A.; Cainelli, G.; Robb, M. A.; Valli, G. S. *J. Org. Chem.* **1993**, *58*, 750.
- Peng, Z.; Merz, K. M., Jr. *J. Am. Chem. Soc.* **1993**, *115*, 9640.
- Pliego, J. R., Jr.; Riveros, J. M. *Chem.—Eur. J.* **2001**, *7*, 169.
- Longo, R. L.; Nunes, R. L.; Bieber, L. W. *J. Braz. Chem. Soc.* **2001**, *12*, 52.
- Zhan, C.-G.; Landry, D. W.; Ornstein, R. L. *J. Phys. Chem. A* **2000**, *104*, 7672.
- Jorgensen, W. L.; Blake, J. F.; Madura, J. D.; Wierschke, S. G. *ACS Symp. Ser.* **1987**, *353*, 200.
- Pliego, J. R., Jr.; Riveros, J. M. *J. Phys. Chem. A* **2002**, *106*, 7434.
- Pliego, J. R., Jr.; Riveros, J. M. *J. Phys. Chem. A* **2001**, *105*, 7241.
- Fuchs, R.; Hagan, C. P.; Rodewald, R. F. *J. Phys. Chem.* **1974**, *78*, 1509.
- Haberfield, P.; Friedman, J.; Pinkston, M. F. *J. Am. Chem. Soc.* **1972**, *94*, 71.
- Roberts, D. D. *J. Org. Chem.* **1965**, *30*, 3516.
- Parker, A. J. *Chem. Rev.* **1969**, *69*, 1.
- Pliego, J. R., Jr.; Riveros, J. M. *Phys. Chem. Chem. Phys.* **2002**, *4*, 1622.
- Pliego, J. R., Jr.; Riveros, J. M. *Chem. Phys. Lett.* **2002**, *355*, 543.
- Ba-Saif, S.; Luthra, A. K.; Williams, A. J. *Am. Chem. Soc.* **1989**, *111*, 2647.
- Jencks, W. P. *Chem. Rev.* **1972**, *72*, 705.
- Shain, S. A.; Kirsch, J. F. *J. Am. Chem. Soc.* **1968**, *90*, 5848.
- Johnson, S. L. *Adv. Phys. Org. Chem.* **1967**, *5*, 237.
- Bender, M. L.; Ginger, R. D.; Unik, J. P. *J. Am. Chem. Soc.* **1958**, *80*, 1044.
- Bender, M. L.; Dewey, R. S. *J. Am. Chem. Soc.* **1956**, *78*, 317.
- Bruice, T. C.; Holmquist, B. *J. Am. Chem. Soc.* **1968**, *90*, 7136.
- Tomasi, J.; Cammi, R.; Mennucci, B.; Cappeli, C.; Corni, S. *Phys. Chem. Chem. Phys.* **2002**, *4*, 5697.
- Tomasi, J.; Cammi, R.; Mennucci, B. *Int. J. Quantum Chem.* **1999**, *75*, 783.
- Barone, V.; Cossi, M.; Tomasi, J. *J. Chem. Phys.* **1997**, *107*, 3210.
- Cances, E.; Mennucci, B.; Tomasi, J. *J. Chem. Phys.* **1997**, *107*, 3032.
- Cossi, M.; Barone, V.; Cammi, R.; Tomasi, J. *Chem. Phys. Lett.* **1996**, *255*, 327.
- Tomasi, J.; Persico, M. *Chem. Rev.* **1994**, *94*, 2027.
- Guthrie, J. P. *J. Am. Chem. Soc.* **1974**, *96*, 3608.
- Slebocka-Tilk, H.; Neverov, A. A.; Brown, R. S. *J. Am. Chem. Soc.* **2003**, *125*, 1851.
- Slebocka-Tilk, H.; Sauriol, F.; Monette, M.; Brown, R. S. *Can. J. Chem.* **2002**, *80*, 1343.
- Almerindo, G. I.; Tondo, D. W.; Pliego, J. R., Jr. *J. Phys. Chem. A* **2004**, *108*, 166.
- Hill, T. L. *An introduction to statistical thermodynamics*; Addison-Wesley: Reading, MA, 1960.
- Miller, W. H.; Handy, N. C.; Adams, J. E. *J. Chem. Phys.* **1980**, *72*, 99.
- Frisch, M. J.; Trucks, G. W.; Schlegel, H. B.; Gill, P. M. W.; Johnson, B. G.; Robb, M. A.; Cheeseman, J. R.; Keith, T.; Petersson, G. A.; Montgomery, J. A.; Raghavachari, K.; Al-Laham, M. A.; Zakrzewski, V. G.; Ortiz, J. V.; Foresman, J. B.; Cioslowski, J.; Stefanov, B. B.; Nanayakkara, A.; Challacombe, M.; Peng, C. Y.; Ayala, P. Y.; Chen, W.; Wong, M. W.; Andres, J. L.; Replogle, E. S.; Gomperts, R.; Martin, R. L.; Fox, D. J.; Binkley, J. S.; Defrees, D. J.; Baker, J.; Stewart, J. P.; Head-Gordon, M.; Gonzalez, C.; Pople, J. A. *Gaussian 94*; Gaussian, Inc.: Pittsburgh, PA, 1994.
- Schmidt, M. W.; Baldrige, K. K.; Boatz, J. A.; Elbert, S. T.; Gordon, M. S.; Jensen, J. H.; Koseki, S.; Matsunaga, N.; Nguyen, K. A.; Su, S.; Windus, T. L.; Dupuis, M.; Montgomery, J. A., Jr. *J. Comput. Chem.* **1993**, *14*, 1347.
- Roux, A.; Perron, G.; Picker, P.; Desnoyers, J. E. *J. Solution Chem.* **1980**, *9*, 59.
- NIST Chemistry WebBook, NIST Standard Reference Database No. 69*; Linstrom, P. J., Mallard, W. G., Eds.; National Institute of Standards and Technology: Gaithersburg, MD 20899, 2003.
- Smith, M. B.; March, J. *March's Advanced Organic Chemistry*; John Wiley & Sons: New York, 2001.
- Mukhtar, T. A.; Koteva, K. P.; Hughes, D. W.; Wright, G. D. *Biochemistry* **2001**, *40*, 8877.
- McMurry, J. *Org. React.* **1976**, *24*, 187.
- Bordwell, F. G. *Acc. Chem. Res.* **1988**, *21*, 456.